

Emmanuel Anane, Annina Sawatzki, Peter Neubauer, Mariano Nicolas Cruz-Bournazou

# Modelling concentration gradients in fed-batch cultivations of *E. coli* – towards the flexible design of scale-down experiments

Journal article | Accepted manuscript (Postprint)

This version is available at <https://doi.org/10.14279/depositonce-8716>



This is the peer reviewed version of the following article:

Anane, E., Sawatzki, A., Neubauer, P., & Cruz-Bournazou, M. N. (2018). Modelling concentration gradients in fed-batch cultivations of *E. coli* - towards the flexible design of scale-down experiments. *Journal of Chemical Technology & Biotechnology*, 94(2), 516–526. <https://doi.org/10.1002/jctb.5798>

which has been published in final form at <https://doi.org/10.1002/jctb.5798>. This article may be used for non-commercial purposes in accordance with Wiley Terms and Conditions for Use of Self-Archived Versions.

## Terms of Use

Copyright applies. A non-exclusive, non-transferable and limited right to use is granted. This document is intended solely for personal, non-commercial use.

**Modelling concentration gradients in fed-batch cultivations of *E. coli* —towards the flexible design of scale-down experiments**

Emmanuel Anane

Annina Sawatzki

Peter Neubauer

Mariano Nicolas Cruz-Bournazou

Chair of Bioprocess Engineering, Institute of Biotechnology, Technische Universität Berlin, Berlin, Germany

**Correspondence:** Dr.-Ing. Mariano Nicolas Cruz Bournazou, Chair of Bioprocess Engineering, Institute of Biotechnology, Technische Universität Berlin, Ackerstraße 76, ACK24, 13355 Berlin, Germany.

**E-mail:** [mariano.n.cruzbournazou@tu-berlin.de](mailto:mariano.n.cruzbournazou@tu-berlin.de)

**Keywords:** *E. coli*, scale-down, glucose gradients, oxygen gradients, modelling, inclusion bodies

**Abstract**

**BACKGROUND:** The impact of concentration gradients in large industrial-scale bioreactors on microbial physiology can be studied in scale-down bioreactors. However, scale-down systems pose several challenges in construction, operation and footprint. Therefore, it is challenging to implement them in emerging technologies for bioprocess development, such as in high throughput cultivation platforms. In this study, a mechanistic model of a two-compartment scale-down bioreactor is developed. Simulations from this model are then used as bases for a pulse-based scale-down bioreactor suitable for application in parallel cultivation systems.

**RESULTS:** As an application, the pulse-based system model was used to study the misincorporation of non-canonical branched-chain amino acids into recombinant pre-proinsulin expressed in *Escherichia coli*, as a response to oscillations in glucose and dissolved oxygen concentrations. The results show significant accumulation of overflow metabolites, up to 18.3 % loss in product yield and up to 10 fold accumulation of the non-canonical amino acids norvaline and norleucine in the product in the pulse-based cultivation, compared to a reference cultivation.

**CONCLUSIONS:** Our results indicate that the combination of a pulse-based scale-down approach with mechanistic models is a very suitable method to test strain robustness and physiological constraints at the early stages of bioprocess development.

## INTRODUCTION

Inadequate mixing and the associated concentration gradients in large-scale microbial bioprocesses have significant impacts on both cell physiology and recombinant protein quality. In these processes, cells are constantly exposed to oscillating concentrations of substrate, metabolites, dissolved oxygen and carbon dioxide. Hence, the study of performance under conditions similar to industrial scale process is essential to increase scale-up reliability and speed up process development.<sup>1,2</sup> The effects of oscillating cultivation conditions on microbial physiology and product yields have been studied in the laboratory by applying scale-down techniques, either in the form of scale-down bioreactors<sup>3-6</sup> or as pulse-based methods.<sup>7-10</sup>

A scale-down system is a laboratory scale bioreactor designed to mimic the environmental conditions in large-scale bioreactors. In multi-compartment scale-down bioreactors, a perfectly mixed stirred tank reactor (STR) is connected to one or more STRs<sup>11</sup> or to one or more plug flow reactors (PFR)<sup>11,12</sup>, through which the culture is circulated at a rate equivalent to a specified residence time (Figure 1A). A stress inducing agent (e.g. highly concentrated substrate, base or acid) is injected into one of the sections, which is eventually mixed with the bulk of the culture in the other sections.<sup>13</sup> In a pulsing system, the stress inducer is injected into the bioreactor intermittently, at specified intervals<sup>7</sup> or randomly<sup>14</sup>. These operation mechanisms produce zones similar to feeding and starvation zones in large-scale bioreactors and result in periodic exposure of the culture to varying stresses.<sup>15</sup> Scale-down techniques have been applied for the successful study of the impact of large-scale gradients for most industrially relevant organisms, with significant differences in process behaviour compared to standard small scale cultivations.<sup>1,12,16,17</sup>

The most recent advances in the development of scale-down concepts include the coupling of computational fluid dynamics (CFD) models of bioreactors with cellular growth kinetics (cellular reaction dynamics, CRD)<sup>18-21</sup> and the mechanistic description of population groups in heterogeneous environments.<sup>22,23</sup> The CFD-CRD models have been used to define specific stress exposure times that are assumed to occur at the larger scale, based on mixing characteristics (CFD simulations) and the dynamics of cellular responses<sup>18</sup>. However, the evaluation of the detailed physiological adaptation to oscillations and their incorporation into CRD models can be an enormous amount of work, as is obvious from the works of Vanrolleghem and Canelas.<sup>24,25</sup> In our opinion, the development of such models and especially their parametrisation could benefit from the parallelization of scale-down systems. Although some authors have applied pulse-based feeding profiles in parallel mini-bioreactor systems<sup>26</sup>, mostly due to the difficulty that continuous feeding

was technically not possible, real scale-down approaches have not been published in parallel systems, to our knowledge.

The objective of this work was to develop a mechanistic model of a typical pulse-based scale-down bioreactor, suitable for application in high throughput parallel cultivation platforms. The mechanistic model of the pulse-based system was developed from simulations of a two-compartment scale-down bioreactor (2CR), which had been used in many studies before. Thus, the principles of two different scale-down concepts (multi-compartment and pulse-based systems) were combined in a mechanistic model to flexibly design the exposure time of the culture to either high or low glucose and oxygen concentrations. The pulse-based system was used to study the influence of model-derived glucose and dissolved oxygen perturbations on the misincorporation of non-canonical amino acids into pre-proinsulin expressed in *E. coli*. The mechanistic modelling concept has the potential to facilitate the incorporation of scale-down studies into experimental set-ups that would already consider scale-up effects at the early stages of bioprocess development. The big benefit is that cellular reaction models which consider the response to oscillations can be developed and parametrised with a much lower effort. Additionally, the run of such experiments in efficient parallel robotic experimental facilities would allow for a rapid phenotyping of large number of candidates under process relevant conditions in short times.<sup>26-29</sup>

## **MATERIALS AND METHODS**

### **Mechanistic Model of Two-compartment Scale-down Bioreactor**

The 2CR system that is modelled in this study has been thoroughly described by Junne et al.<sup>30</sup> It consists of a 12 L (working volume) stirred tank bioreactor connected to a 1.2 L plug flow reactor. Using the ratio of the volumes of the PFR:STR and the feed and recycling rates, it is estimated that a cell, on average, spends about 5 min in the STR before going through one cycle in the PFR, if the residence time in the PFR is set to 30 seconds.<sup>30</sup> The mathematical model used to describe the macro-kinetic dynamics of the culture has been presented elsewhere,<sup>31</sup> but a summarized version is presented in the Appendix. This model is a nonlinear Ordinary Differential Equation (ODE) system given as:

$$\begin{aligned}
\dot{x}(t) &= f(x(t), u(t); \theta) \\
x(t_0) &= x_0 \\
y(t) &= A x(t)
\end{aligned}
\tag{1}$$

where  $t \in [t_o, t_{end}] \subseteq \mathbb{R}$  is the time,  $x(t) \in \mathbb{R}^{n_x}$  are dependent state variables,  $u(t) \in \mathbb{R}^{n_u}$  are the time-varying inputs or experimental design variables,  $\theta \in \mathbb{R}^{n_p}$  the unknown parameter vector, and initial conditions are given by  $x_0$ . The vector  $y(t) \in \mathbb{R}^{n_y}$  are the predicted response variables whose elements are defined by the selection matrix  $A \in \mathbb{R}^{n_y \times n_x}$ . The states considered are the biomass concentration (X, g L<sup>-1</sup>), glucose as substrate concentration (S, g L<sup>-1</sup>), extracellular acetate concentration (A, g L<sup>-1</sup>), and dissolved oxygen tension (DOT in % of saturation).

Some important assumptions have to be made to achieve the required level of simplification in the model of the two-compartment reactor, which have to be considered:

- I. There is no cell history (the cultivation can be described by a time invariant equation system)
- II. The metabolic activity under anaerobic conditions can be tracked by changes in parameter values of the model
- III. The STR is ideally mixed so that there is no distribution in the residence time of the microorganisms
- IV. the PFR has no concentration gradients in radial direction, and convection and diffusion effects can be neglected.

The 2CR model is complicated by the fact that the plug flow reactor never reaches steady state because of the continuous recycling of broth from the STR and the exponential feed injected into the PFR section (Figure 1A). To formulate the mechanistic model of the 2CR system, the transient solution of the Partial Differential Equation (PDE) system was solved by finite differences with discretization in space (dividing the 3.6 m long PFR into 100 tiny reactors), and solving the biomass, glucose, acetate and dissolved oxygen (DOT) profiles of the *E. coli* model<sup>31</sup> over each finite element. The cumulative time of the transient solution is equal to the desired residence time in the PFR. By varying the flow rate of the recycling stream in the simulations, different residence times, and therefore different biomass and glucose profiles can be achieved in the PFR (Figure 2). This can then be used to judge how long the culture has been exposed to the stressing agent (e.g. glucose), as demonstrated in

the simulations of a single cell trajectory (Figure 1 C) for a cell that moves through both the stirred tank and plug flow reactors. The trajectory of an average cell is calculated as

$$v(t) = F(t)/A \quad (1)$$

where  $v(t)$  represents the velocity of the cell ( $\text{m h}^{-1}$ ),  $F(t)$  represents the feed flow rate ( $\text{m}^3 \text{h}^{-1}$ ), and  $A$  the cross-sectional area of the PFR. In order to facilitate the computation of the trajectory including the volume change in the STR due to feeding, the geometry of the 2CR is transformed into a toroid with an ideally mixed flow (Figure 1C, top). The volume ratios of STR:PFR and feeding points in the actual 2CR and the toroidal shape are equal. The varying glucose concentrations a traversing cell is exposed to between the STR and PFR are equivalent to intermittent glucose pulses (Figure 1C, bottom). Therefore, to transfer these characteristics to a pure glucose pulsing scheme, simulations were done to determine the  $\tau$ ,  $\mu_{\text{set}}$  and feed concentrations at which there would be a glucose carry over from the PFR into the STR. This would ensure the maximum exposure time to the stress in the pulse-based scale-down system.

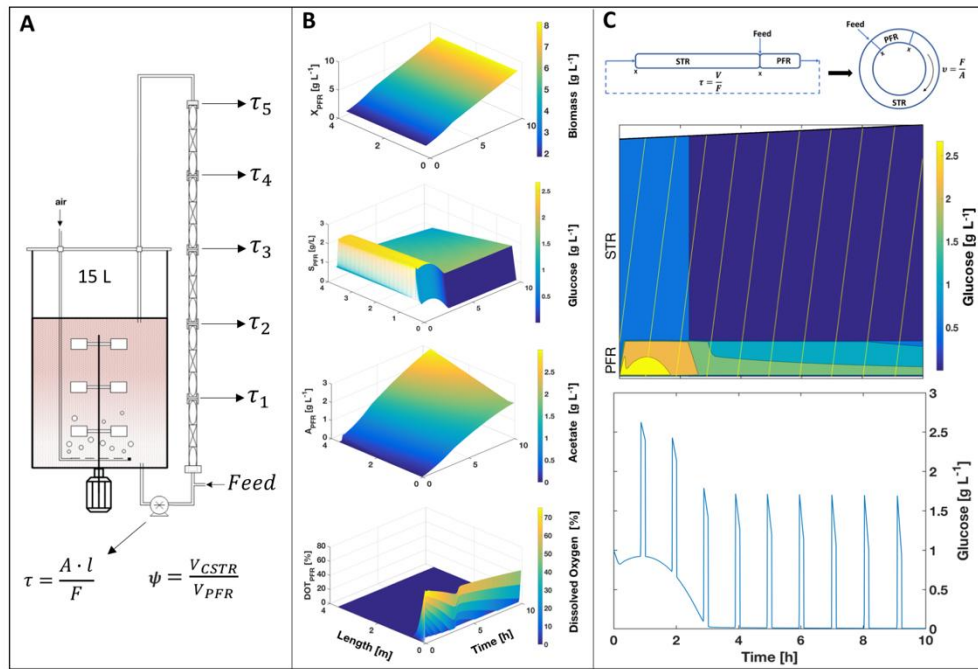


**Figure 1 (A)** Schematic diagram of two-compartment bioreactor consisting of a stirred tank reactor and a plug-flow reactor. **(B)** Profiles of dissolved oxygen, biomass, glucose and acetate after running the 2CR for 10 hours with feed injection into the PFR **(C) top:** Cascade configuration of 2CR and toroidal conversion for calculation of cell trajectories; *middle:* Gradient profiles of glucose showing the trajectory of a single cell and the glucose concentrations it encounters as it circulates between the STR and PFR; *bottom:* pulse representation of glucose gradients experienced by one cell (Glucose in feed =  $250 \text{ g L}^{-1}$ ,

biomass in STR = 1.85 g L<sup>-1</sup> dry weight—Matlab code and full details of simulation are available in the Supplementary Material).

### **Recycling Rate in the PFR**

The recycling rate is determined by the flow rate set on the recycling pump (Figure 1 A). The recycling rate of the broth determines three important factors of the 2CR: (i) the duration of the stress, i.e. time in which the culture is exposed to excess glucose environments, (ii) the magnitude of the stress, i.e. the strength of concentration gradients and (iii) the number of times a particular cell goes through a cycle in the PFR, which is the frequency of exposure to the stress. When the exposure time is in the same or a few orders of magnitude as the characteristic growth time ( $1/\mu$ ), there is a marked influence of the stress on both physiological and metabolic, as well as transcriptional processes in the cell<sup>8,17,32</sup>. Therefore, it is important to determine, in the simulations of the 2CR, how the recycling rate affects both the frequency and magnitude of glucose gradients that the cells are exposed to. These profiles are shown in Figure 2. At low recycling rates, the cells spend a longer time in the PFR and are therefore exposed to a stronger pulse (higher magnitude, low frequency). At higher recycling rate, the pulse size is smaller, but the cell passes through the vicinity of the stress many times within a given period.



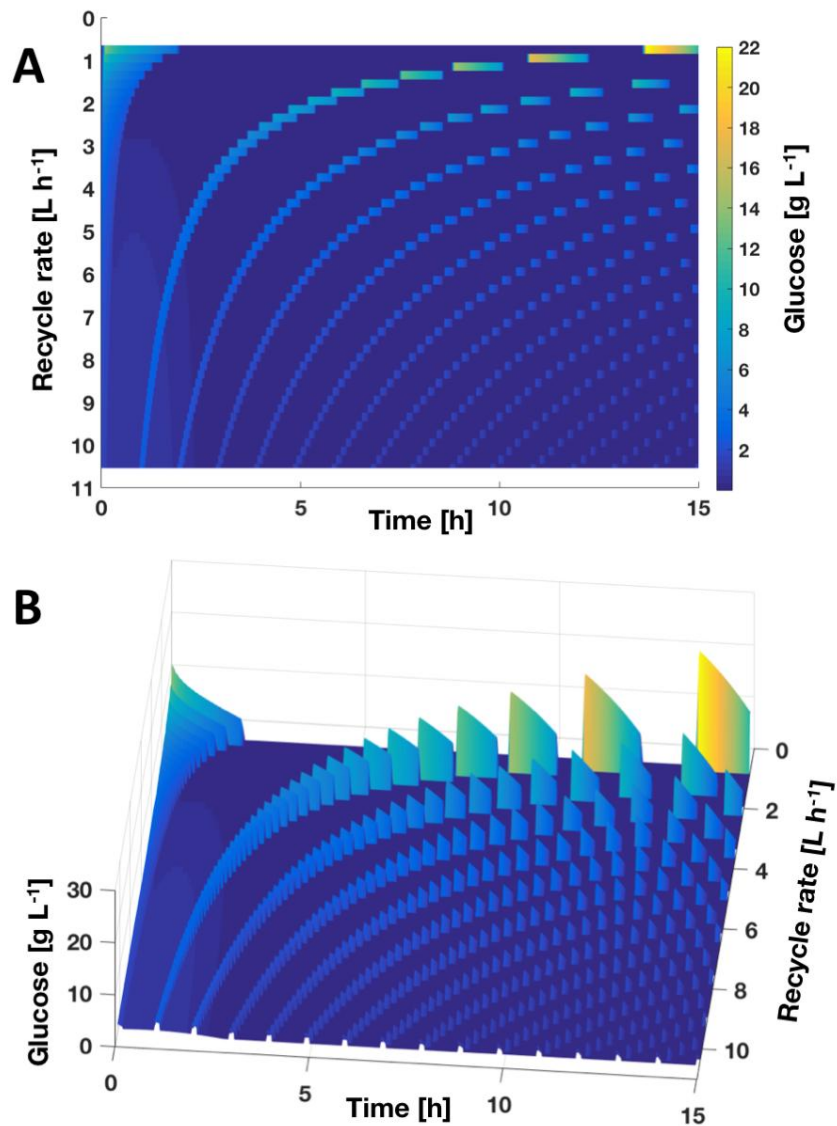


**Figure 2** Effect of recycling rate on (A) pulse frequency and (B) pulse size. High recycling rates result in high frequency of exposure, but at lower gradient sizes, and vice versa.

### Strain and Fermentation Conditions

All experiments were performed with *E. coli* W3110M (*lacI<sup>q</sup>*) pSW3 (*amp<sup>r</sup>*)<sup>33</sup> expressing a recombinant mini-proinsulin under a *tac*-promoter (inducible with IPTG) (kindly provided by Sanofi-Aventis Deutschland GmbH) in a 3.7 L bioreactor (KLF 2000, Bioengineering AG, Wald, Switzerland). As pre-culture, 25 ml of bioreactor medium was inoculated with stock cultures of this strain in a 125 ml Erlenmeyer flask and incubated at 37 °C, 250 rpm in an orbital shaker (Adolf Kühner AG, Birsfelden, Switzerland). After 12 hours, appropriate volumes of the pre-culture were used to inoculate the bioreactor to an OD<sub>600</sub> of 0.01. The bioreactor medium consisted of mineral salt medium, containing (per

L): 2 g Na<sub>2</sub>SO<sub>4</sub>, 2.468 g (NH<sub>4</sub>)<sub>2</sub>SO<sub>4</sub>, 0.5 g NH<sub>4</sub>Cl, 14.6 g K<sub>2</sub>HPO<sub>4</sub>, 3.6 g NaH<sub>2</sub>PO<sub>4</sub> × 2H<sub>2</sub>O, 1 g (NH<sub>4</sub>)<sub>2</sub>-H-citrate and 1 ml antifoam (Antifoam 204, Sigma). Before inoculation, the medium was supplemented with 2 ml L<sup>-1</sup> trace elements solution, 2 ml L<sup>-1</sup> MgSO<sub>4</sub> solution (1.0 M) and 1 ml L<sup>-1</sup> ampicillin (100 mg L<sup>-1</sup>). The trace element solution comprised (per L): 0.5 g CaCl<sub>2</sub> × 2H<sub>2</sub>O, 0.18 g ZnSO<sub>4</sub> × 7H<sub>2</sub>O, 0.1 g MnSO<sub>4</sub> × H<sub>2</sub>O, 20.1 g Na-EDTA, 16.7g FeCl<sub>3</sub> × 6H<sub>2</sub>O, 0.16 g CuSO<sub>4</sub> × 5H<sub>2</sub>O, 0.18 g CoCl<sub>2</sub> × 6H<sub>2</sub>O. In all bioreactor cultivations, the initial glucose concentration for the batch phase was 5 g L<sup>-1</sup>. The temperature was maintained at 37 °C and the pH was controlled at 7 by automatic titration with 25% NH<sub>4</sub>OH solution.

### Reference Cultivation

At the end of the batch phase, an exponential feeding mechanism was implemented in the reference cultivation according to Equation 1,

$$F(t) = \frac{\mu_{set}}{Y_{x/s}S_i}(XV)e^{\mu_{set}(t-t_b)} \quad (2)$$

where F represents the feed flow rate (L h<sup>-1</sup>), S<sub>i</sub> (g L<sup>-1</sup>) the concentration of glucose in the feed, Y<sub>x/s</sub> the biomass yield coefficient (g g<sup>-1</sup>), μ<sub>set</sub> the set-point of the specific growth rate (h<sup>-1</sup>) and t<sub>b</sub> the time at which the batch phase ended. After three hours of exponential feeding, recombinant protein production was induced by a pulse addition of IPTG to a final concentration of 1 mM. The feed was then switched to a constant feed, where the constant flow rate was equal to the last flow rate reached in the exponential feeding phase. The feed solution contained 8 ml L<sup>-1</sup> trace elements solution, mineral salts (same concentration as in batch phase) and 400 g L<sup>-1</sup> glucose.

A mass balance on gases across the entry and exit points on the STR was used to calculate the specific oxygen consumption rate (qO<sub>2</sub>) and specific carbon dioxide evolution rate (qCO<sub>2</sub>) as

$$q_{O_2} = V_G(O_2in - \{O_2out \times (N_2in/N_2out)\})/X \quad (3)$$

$$q_{CO_2} = V_G(\{CO_2out \times (N_2in/N_2out)\} - CO_2in)/X \quad (4)$$

where V<sub>G</sub> represents the gassing rate (mol L<sup>-1</sup> h<sup>-1</sup>) and X the biomass concentration (g L<sup>-1</sup>). The concentration of all gases in Equations 2 and 3 are in volumetric fractions (%v v<sup>-1</sup>) and were determined by measuring the composition of the exhaust gas using a BlueSens off-gas analyser (BlueSens Gas Sensor GmbH, Herten, Germany). The biomass concentration for each off-gas measuring point was determined by fitting a biomass profile to values of hourly samples, and interpolating at off-gas measuring points. The respiratory quotient was calculated as  $RQ = q_{CO_2}/q_{O_2}$ .

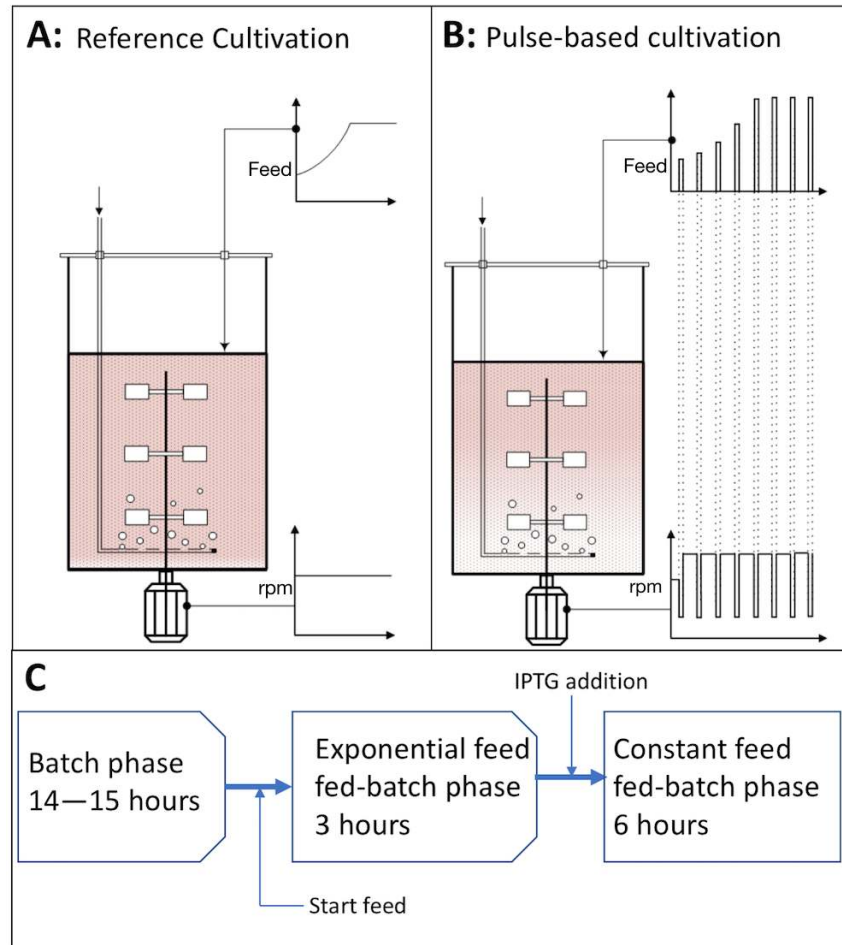


**Figure 3** Schematic diagram of (A) the reference cultivation showing the constant agitation rate (lower curve) and the smooth glucose feed in two phases: exponential feed followed by constant feeding (upper curve), (B) the pulse-based cultivation showing the intermittent supply of glucose feed as pulses in both the exponential and constant feeding phases. The glucose pulses coincide with rpm shifts to achieve the desired gradients; (C) overall cultivation scheme.

### Pulse-based Cultivation

In order to mimic the oscillations in DOT and glucose concentrations of large industrial-scale bioreactors in the pulse-based system, the calculated exponential feed (Equation 1) at the end of the batch phase was divided into discrete pulses of 1 min feeding followed by 9 min of glucose limitation as determined from the 2CR simulations. The amount of glucose fed within the 1 min was equal to that which would have been fed in a continuous exponential feed for 10 min (1+9), to maintain the set point of the specific growth rate at  $0.25 \text{ h}^{-1}$ . During the 1 min feeding period, the agitation rate was manually

decreased to 400 rpm, (from 800 rpm in the batch phase). In the glucose-limiting phase, it was increased to 1000 rpm (Figure 3). These cyclic shifts resulted in recurring oxygen-rich and oxygen-deficient conditions, which, together with the glucose pulses, resulted in approximate oscillations in concentration as observed in the 2CR system and in large-scale. The feed switching was done manually by turning the feed pump on and off, as required. The kinetics of glucose consumption and acetate production during glucose pulsing were followed by rapidly sampling through a 0.22  $\mu\text{m}$  filter at the point of glucose addition (0 seconds), 1 min, 3 min and 6 min after each pulse. A total of 3 pulses were sampled: two in the exponential feeding phase and one after protein induction. The effect of environmental oscillations on overall growth kinetics, cell mass and the accumulation of metabolites and non-canonical branched chain amino acids in the recombinant protein product were assessed by analysing hourly samples. The Respiratory Quotient (RQ) was calculated for the pulsed-based cultivation as in the reference cultivation. Recombinant protein production was induced by adding IPTG to the same concentration as in the reference cultivation.

### **Analyses**

Cell growth was monitored in both the reference and pulse-based cultivations by measuring the optical density of samples in a UV-vis spectrophotometer (Novaspec III, Amersham Biosciences, Amersham, UK) in triplicate, at a wavelength of 600 nm ( $\text{OD}_{600}$ ). The dry weight was calculated from the  $\text{OD}_{600}$  values, using a conversion factor of 0.37 g L<sup>-1</sup> dry weight per  $\text{OD}_{600}$ , which was previously established for this strain using the same spectrophotometer. Supernatant samples for analysis of residual glucose and acetate were taken from the bioreactor through a 0.22  $\mu\text{m}$  membrane filter at the sampling port and stored at -20 °C for further analysis. The concentration of organic acids and glucose were measured with an Agilent 1200 HPLC system (Waldbronn, Germany), equipped with a HyperRez™ XP Carbohydrate H+ column (300 × 7.7 mm, 8  $\mu\text{m}$ ) (Fisher Scientific, Schwerte, Germany) and a refractive index detector, using 5 mM H<sub>2</sub>SO<sub>4</sub> as the eluent at a flow rate of 0.5 ml min<sup>-1</sup>. The column temperature was set to 65 °C.

For analysis of the recombinant protein, samples were taken from the bioreactor every hour after protein induction. These samples were normalized to  $\text{OD}_{600} = 15$  (in 1 ml) and centrifuged at 16000 ×g for 5 min in pre-weighed Eppendorf tubes. The cell pellet was weighed and stored at 4 °C for inclusion body (IB) purification. The inclusion body separation was carried out with Bugbuster® protein extraction kit (Novagen, Darmstadt, Germany) as follows. The cell pellets from the normalized samples were resuspended in

Bugbuster® reagent and incubated for 20 min at room temperature, taking 5 ml of reagent per gram of wet cell paste. To reduce the viscosity and improve inclusion body extraction, 25 units of benzonase and 1000 units of rLysozyme™ (all from Merck KGaA, Darmstadt, Germany) were added, for each millilitre of Bugbuster reagent used. After the incubation period, the samples were centrifuged and the pellets washed 3 times in 10× diluted Bugbuster reagent to obtain the purified inclusion bodies. The mass of inclusion bodies per mass of biomass was used as quantitative measure of the inclusion body fraction. All the purified inclusion bodies obtained from Bugbuster method and 125 µL of internal standard (0.225 mM α-aminobutyric acid) were hydrolysed in 1 ml of 6 M HCl at 80 °C for 24 h. The hydrolysed samples were then dried in a speed vacuum concentrator (Bachhofer, Reutlingen, Germany), followed by derivatization of the solid residue at 60 °C for 60 min. The derivatization reagents were 50 µL N-(tert-butyltrimethylsilyl)-N-methyl-trifluoroacetamide (MTBSTFA), 50 µL acetonitrile and 5 µL anhydrous 1-butanol (all from Merck KGaA, Darmstadt, Germany). The derivatized samples were analysed on an Agilent 5975C GC-MS system equipped with a DB-5MS column (30 m × 250 µm, 0.25 µM) and a quadrupole detector, using helium as the carrier gas. All amino acid concentrations were normalized to the mass of inclusion bodies that was hydrolysed.

## RESULTS

### Model Fitting of the Pulse-Based System

The dynamic model which was used to derive the glucose pulses was fitted to the pulse feeding experiment to allow a better understanding of growth kinetics under oscillating environmental conditions. The model parameters were estimated by solving the optimization problem

$$\hat{\theta} := \arg \min_{\theta} \Phi(U, \theta) \quad (5)$$

where the nonlinear least-square objective function  $\Phi(U, \theta)$  was calculated as

$$\Phi(U, \theta) := \frac{1}{2} (Y(U, \theta) - Y^m)^T (Y(U, \theta) - Y^m) \quad (6)$$

In equation 6,  $Y(U, \theta)$  represents the model predictions whereas  $Y^m$  represents the experimental data. Both the exponential feeding and constant feeding phases of the pulse-based cultivation and the corresponding model fitting are shown in Figure 4, with dynamic response of the state variables to oscillating glucose input. The recently described mechanistic model<sup>31</sup> was solved in a pulsing manner, with the addition of residence times of the PFR to dictate the frequency of the pulses. The model fitting

resulted in a set of parameter values that sufficiently describe growth under glucose and dissolved oxygen stresses. The model solution fits the experimental data to acceptable accuracy, as given by the relative standard deviations (<20 %) of the estimated parameters (Table 1). In further applications, the estimated model parameters can be used to calculate various pulse sizes at varying frequencies, as a means of studying gradient effects under different process conditions.

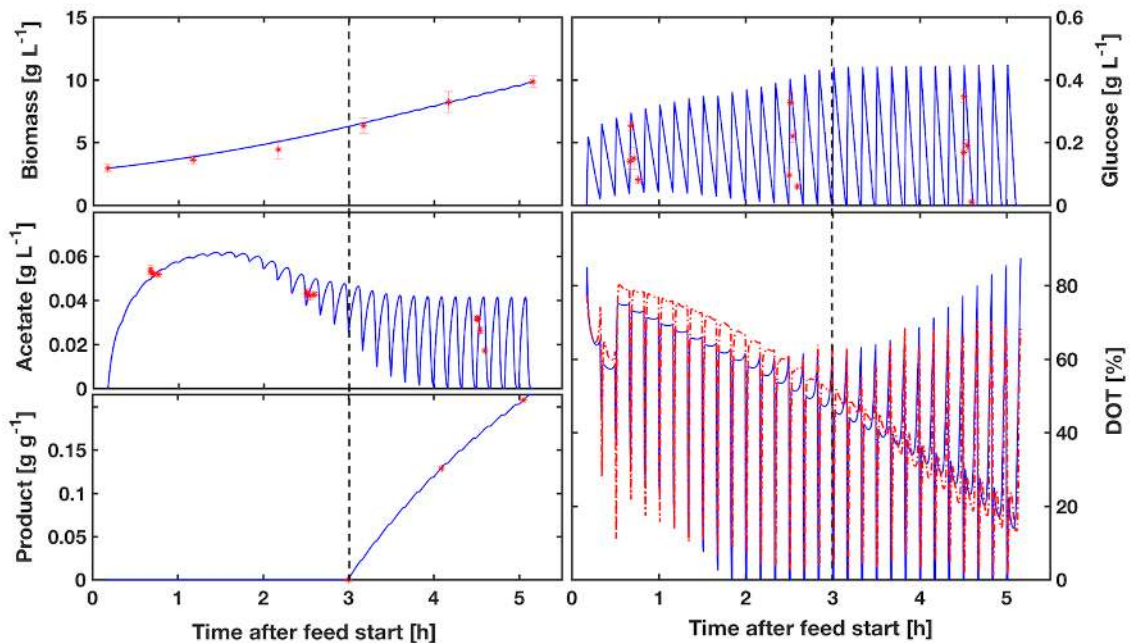


**Figure 4** Model fitting of fed-batch phase of the pulse-based scale down cultivation (experimental data \*, model — ). The dashed line represents the time of induction (3h). The Matlab code for the model fitting is available as a Supplementary Material.

### Growth and Metabolic Behaviour in Pulse-based and Reference Cultivations

Although the pulse-based experiment and the reference cultivation had similar biomass concentrations at the end of their respective batch phases, they showed different growth patterns during the exponential feeding phase, with the reference cultivation reaching 15 % less biomass than the pulse cultivation at the end of this phase. The specific growth rate  $\mu$  achieved in the exponential feeding phase in the pulse-based cultivation was slightly lower (average of  $0.23 \text{ h}^{-1}$ ) than in the reference cultivation ( $0.24 \text{ h}^{-1}$ ), compared to the set point of  $\mu_{\text{set}} = 0.25 \text{ h}^{-1}$ . Upon changing from exponential feed to constant feed with protein induction, the specific growth rates declined (Figure 5C) with the decreasing supply of glucose per gram of biomass. However, the pulse-based culture sustained some level of

growth (biomass profile, Figure 5A), leading to a more gentle, exponential decline in  $\mu$ , compared to a sharper decline in  $\mu$  for the reference cultivation.

**Table 1.** Results of model fitting for pulse-based scale-down experiments

Par	Unit	Initial* guess	Estimate	Standard Dev		95% CI	
			$\hat{\theta}_1$	$\sigma$	% $\sigma$	LB	UB
$K_{ap}$	$g\ g^{-1}\ h^{-1}$	0.438	0.349	0.029	8.30	0.340	0.3570
$K_{sa}$	$g\ L^{-1}$	0.016	0.020	0.003	15.0	0.019	0.0210
$K_s$	$g\ L^{-1}$	0.035	0.019	0.003	15.7	0.0182	0.0198
$K_{is}$	$g\ L^{-1}$	1.111	14.26	1.338	9.40	13.890	14.629
$K_{ip}$	$g\ g^{-1}$	1.562	0.870	0.108	12.4	0.835	0.9051
$\rho_{Amax}$	$g\ g^{-1}\ h^{-1}$	0.203	0.326	0.041	12.6	0.3150	0.3274
$q_{Amax}$	$g\ g^{-1}\ h^{-1}$	0.106	0.250	0.026	10.1	0.2428	0.2572
$q_m$	$g\ g^{-1}\ h^{-1}$	0.013	0.040	0.001	2.40	0.0397	0.0403
$q_{Smax}$	$g\ g^{-1}\ h^{-1}$	0.635	0.519	0.025	4.80	0.5121	0.5259
$Y_{as}$	$g\ g^{-1}$	0.827	0.970	0.203	20.9	0.9039	0.9999
$Y_{oa}$	$g\ g^{-1}$	1.100	1.199	0.101	8.42	1.1710	1.2270
$Y_{xa}$	$g\ g^{-1}$	0.611	0.501	0.091	18.2	0.4760	0.5260
$Y_{em}$	$g\ g^{-1}$	0.546	0.481	0.134	20.8	0.4440	0.5187
$Y_{os}$	$g\ g^{-1}$	1.100	1.079	0.073	6.80	1.0530	1.0930
$Y_{xsof}$	$g\ g^{-1}$	0.206	0.351	0.041	11.7	0.3399	0.3620
$Y_{px}$	$g\ g^{-1}$	0.250	0.532	0.039	7.40	0.5211	0.5434

\*initial parameter guesses taken from literature <sup>26,31</sup>

In the pulse-based cultivation, all the glucose in a pulse was consumed before the end of the 10 min interval, indicated by a sharp increase in DOT, 60 to 80 seconds before the next glucose pulse (Figure 4) during the constant feeding phase. Considering that this pulse contained the same amount of glucose as in ten min of continuous feed in the reference cultivation, the pulse-based cultivation seemed to have a higher specific glucose uptake rate than in the reference cultivation. As the major product of overflow metabolism in *E. coli*, acetate accumulated to higher levels in the pulse-based system than in the reference cultivation. After the change to constant feeding, acetate was immediately re-assimilated

in the reference cultivation, but acetate re-assimilation in the pulse-based system was delayed up to 1 hour after protein induction (Figure 5B).

The RQ remained constant at around 1.2 for the reference cultivation as shown in Figure 4D. The RQ for the pulse cultivation shows the periodic availability and depletion of glucose in response to the pulses, with an average value (middle line, Figure 5D) that declined continuously in the course of the cultivation from 1.48 to 1.05 at the end. In the analysis of *E. coli* cultures growing on glucose, the RQ value is unaffected by overflow metabolism due to the fact that the substrate (glucose), the major overflow product (acetate) and the biomass all have the same degree of reduction of approximately 4.<sup>14,34</sup> Therefore, the RQ value is not as informative in *E. coli* as it is in cultivations of *Saccharomyces cerevisiae* where it can indicate important overflow metabolic states due to differences between the degree of reduction of glucose and that of ethanol. However, in the pulse-based cultivation, the intermittent exposure of the culture to anaerobic conditions can lead to the formation of formate and lactate which should have an influence on the cumulative degree of reduction of the metabolites. Therefore, the metabolic behaviour showed a slightly higher average RQ value for the reference cultivation than in the pulse-based cultivation during recombinant protein production.

### **Inclusion Body Formation and Recombinant Product Quality**

Prior to protein induction by IPTG in the pulse-based cultivation, there was already some accumulation of inclusion bodies in the cells (Figure 6A). This seemingly leaky expression, which was not observed in the reference cultivation can be attributed to the partial de-repression of the *tac* promoter by the intermittent glucose limitation<sup>35</sup> between pulses in the exponential feeding phase. As shown in Figure 6A, the pulse based scale-down cultivation condition led to a lower amount of recombinant pre-proinsulin per gram of biomass than in the reference cultivation. The final product yield in the pulse-based cultivation was 18 % lower than in the reference cultivation.

The quality of the recombinant product, as used in this text refers to the concentration of non-conventional amino acids (norvaline, norleucine and beta-methyl-norleucine) present in the purified product. These amino acids replace their corresponding canonical forms (leucine, methionine and isoleucine, respectively) in the product under stressful cultivation conditions<sup>36</sup> and thus reduce the efficacy of therapeutic proteins produced recombinantly in *E. coli*. The results of the scale-down studies show a steady increase in the concentration of non-canonical amino acids in the product for the pulse-based



cultivation, which is about 10-fold higher than their concentrations in the reference cultivation.

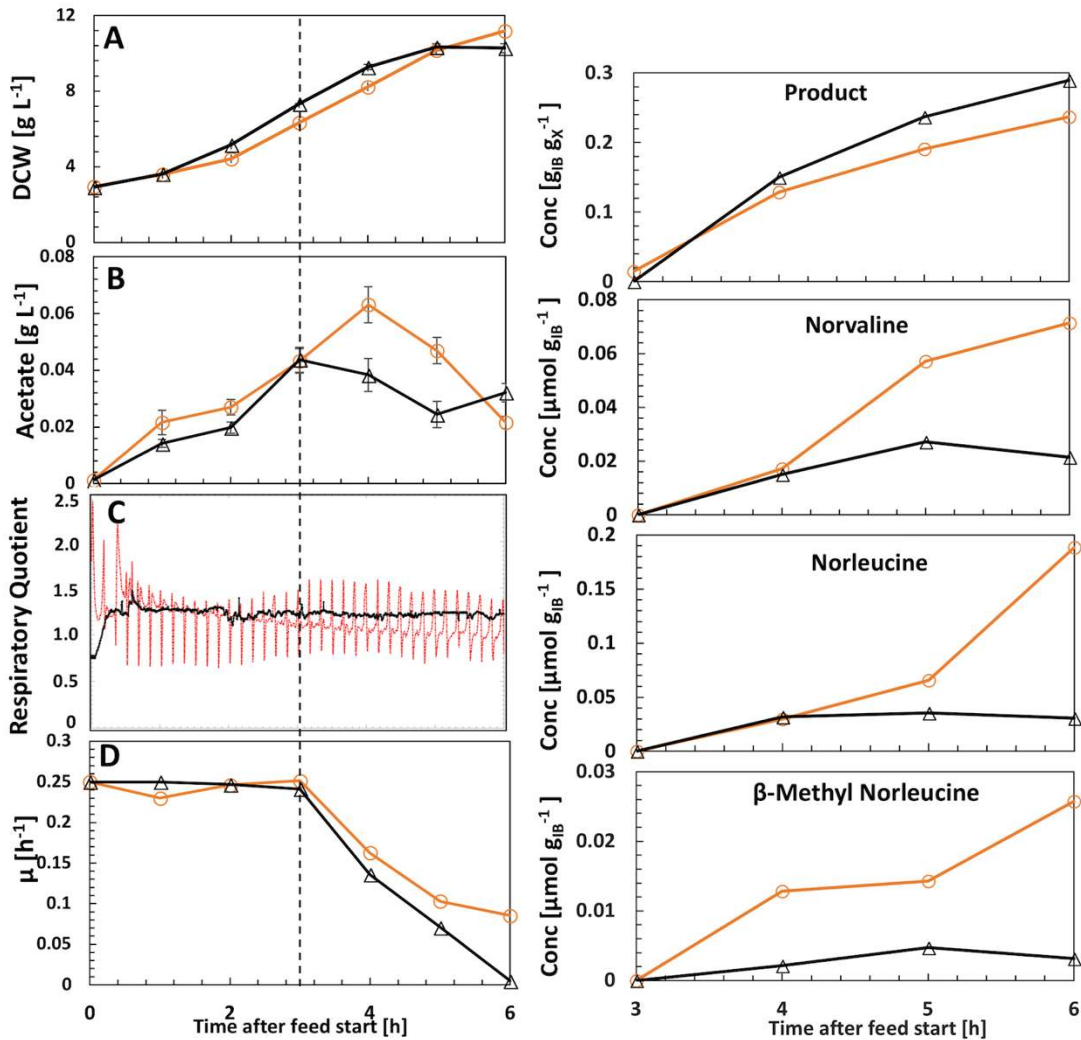


**Figure 5 (Left)** Growth profiles and metabolic activity of *E. coli* during the fed-batch phase of cultivations under pulse-based (O) and reference cultivation ( $\Delta$ ) methods. **(A)** Biomass concentration, **(B)** Extracellular acetate concentration, **(C)** Respiratory quotient and **(D)** Specific growth rate during the exponential and constant feed fed-batch phases. The dashed line indicates the point of induction by IPTG. Error bars show the standard deviation. **Figure 6 (Right)** Product formation profile and the concentration of non-canonical amino acids in the purified inclusion bodies from the pulse-based cultivation (O) and the reference cultivation ( $\Delta$ ).

## DISCUSSION

### Physiological Response of *E. coli* to Glucose and Oxygen Pulses

Scale-down bioreactors provide an effective method to investigate the challenges of bioprocess scale-up. Their ability to mimic the environmental heterogeneity in large-scale bioreactors provides a possibility to look into the dynamics of industrial cultivations, and to study the effects of such dynamics on microbial physiology and process efficiency. The model-based pulsing scheme implemented in the current study as a scale-down methodology resulted in significant differences in both the metabolic behaviour and recombinant protein quality, compared to the reference cultivation. Earlier studies report that *E. coli* cells in oscillating environmental conditions show a higher cell viability in comparison to laboratory-scale cultivations.<sup>5,15</sup> This observation was also confirmed in the current study as seen in the more gentle decline of specific growth rate for the scale-down cultivation (Figure 5C). This higher viability can be attributed to the higher specific uptake capacities under oscillating conditions, as observed in the glucose uptake rates in the current study and also discussed by Lin et al.<sup>37</sup> The loss of product yield in heterogeneous conditions is a common occurrence during bioprocess scale-up.<sup>38,39</sup> The results of the scale-down cultivation indicate a significant loss in product yield in the presence of heterogeneous environmental conditions. This lower product accumulation rate (Figure 5B) may be due to the loss of valuable carbon source through overflow metabolism and the associated low ATP generation under stressful cultivation conditions.<sup>10</sup> These factors lead to a lower biomass accumulation rate and consequently, a lower specific product formation rate in large-scale bioreactors, as demonstrated in the scale-down cultivation in the present study.

There was also a significant accumulation of non-canonical amino acids in the purified inclusion bodies in the pulse-based cultivation. According to recent reviews,<sup>36,40</sup> these wrong amino acids can arise from metabolic by-products originating from environmental stresses in *E. coli* cultivation. The results of Soini et al. (2008) also directly link heterogeneous fermentation conditions to norvaline accumulation in *E. coli* W3110.<sup>41</sup> Thus, the higher accumulation of these non-canonical amino acids in the pulse-based cultivation shows the ability of this cultivation set-up to reproduce environmental stresses that trigger unfavourable responses in *E. coli*, under scale-down conditions.

### Model Application in Scale-down Bioreactor Systems

A major outcome of the current study is the dynamic description of concentration gradients in a mechanistic framework, that allows the estimation of physiological

parameters under oscillating environmental conditions. These parameters, when estimated in high throughput platforms under scale-down conditions can be used for CFD-CRD applications, <sup>21,42</sup> as well as for screening large libraries under real cultivation conditions. The application of glucose pulses for physiological studies in fermentation is not a new concept. <sup>7,14</sup> However, in most of the previous studies the pulses applied were randomly determined and not based on any physiological basis. Here, an exponential feed profile to maintain a certain specific growth rate in the fed-batch phase was calculated, then a mechanistic model (see pseudocode in Supplementary material) was used to discretize this feed into pulses according to gradient profiles simulated in the 2CR. The duration, frequency and magnitude of concentration gradients in an actual large-scale bioreactor are all dynamic parameters. <sup>15,43</sup> In effect, the exposure time in the scale-down bioreactor should be a flexible parameter that can be changed easily, to suit a specific large-scale bioreactor. <sup>44</sup> In the current contribution, this flexibility of scale-down design is offered by the modelling framework of the pulse-based system. Thus, data for the inclusion of variable exposure times to study response kinetics of specific zones (organism lifelines) in CFD-CRD models can be generated easily in such an experimental set-up. Although the pulse-based feed leads to a synchronised response of the culture to the stress, advanced process analytical technology (PAT) tools such as online in-situ microscopy <sup>45</sup> could be used to monitor the population heterogeneity.

## **CONCLUSIONS**

We have demonstrated in this study that physiological behaviour of cells under environmental oscillations can be described fully with mechanistic models. The model can then be used to design simple scale-down experimental setups, which is a step in simplifying scale-down bioreactor systems for application in parallelization. Such experimental set-ups could be used to study the effects of scale-up stresses on the efficiency of bioprocesses at the early stages of process development. As demonstrated by Cruz et al. <sup>26</sup>, model-based automation can be used to achieve faster bioprocess characterization. Therefore, incorporating scale-up effects into such platforms through modelling provides further opportunities to facilitate bioprocess development with scale-up in mind.

## **ACKNOWLEDGEMENTS**

We are grateful for financial support from the European Union's Horizon 2020 research and innovation program under the Marie Skłodowska-Curie actions grant agreement No. 643056 (Biorapid).

### Conflict of interest

The authors declare no financial or commercial conflict of interest.

### Supplementary Data

The Matlab® codes and fermentation data can be found at [https://gitlab.tubit.tu-berlin.de/nicolas.cruz/E\\_coli\\_fed-batch/tree/master/Anane\\_2018\\_ICTB](https://gitlab.tubit.tu-berlin.de/nicolas.cruz/E_coli_fed-batch/tree/master/Anane_2018_ICTB)

### Appendix

#### Macro-kinetic model of *Escherichia coli*

The mechanistic model of *E. coli* used in this publication is based on the physiological use of glucose, in a glucose partitioning framework as well as the overflow of glucose to acetate through the acetate cycling concept. The two physiological concepts, as given by Neubauer et al. 2000<sup>9</sup> and Lin et al.,<sup>37</sup> and basic growth concepts such as Monod kinetics and acetate inhibition are used to derive simple algebraic equations that describe intracellular pathways of glucose and oxygen usage. Details on the derivation of the model and its subsequent usage in *E. coli* processes can be found in the literature.<sup>26,31,37</sup> The algebraic equations that describe these intracellular activities are as follows:

$$q_s = \frac{q_{smax}S}{S+K_s} \cdot e^{-P \cdot K_{ip}} \quad (A.1)$$

$$q_{sox} = \left( q_s - \frac{P_{Amax}q_s}{q_s+K_{ap}} \right) \cdot \frac{DOT}{DOT+K_o} \quad (A.2)$$

$$q_{sof} = q_s - q_{sox} \quad (A.3)$$

$$p_A = q_{sof}Y_{as} \quad (A.4)$$

$$q_{sA} = \frac{q_{Amax}}{1 + \frac{q_s}{K_{is}}} \cdot \frac{A}{A+K_{sa}} \quad (A.5)$$

$$q_A = p_A - q_{sA} \quad (\text{A.6})$$

$$\mu = (q_{sox} - q_m)Y_{em} + q_{sA}Y_{xa} + (q_{sof} - p_A)Y_{xsof} \quad (\text{A.7})$$

$$q_o = (q_{sox} - q_m)Y_{os} + q_{sA}Y_{oa} \quad (\text{A.8})$$

$$q_p = \mu Y_{px} \quad (\text{A.9})$$

The algebraic equations are coupled with mass balances for a fed-batch process to yield the full ODE system. The ODE system for the *E. coli* mechanistic model is derived from mass balances on biomass (X), glucose (substrate, S), acetate (A) and dissolved oxygen measured as the percentage saturation at the operating conditions in the bioreactor (DOT).

$$\frac{dX}{dt} = \frac{F}{V}(0 - X) + \mu X \quad (\text{A.10})$$

$$\frac{dS}{dt} = \frac{F}{V}(S_i - S) - q_s X \quad (\text{A.11})$$

$$\frac{dA}{dt} = \frac{F}{V}(0 - A) + q_{sA} X \quad (\text{A.12})$$

$$\frac{dDOT}{dt} = K_{La}(DOT^* - DOT) - q_o X H \quad (\text{A.13})$$

$$\frac{dP}{dt} = q_p - \mu P \quad (\text{A.14})$$

The model (equations A.1—A.14) was compiled as a single mathematical function (e\_colimodel) and implemented in Matlab® R2016a. The model was integrated with ode15s solver and parameter estimation was done with the *fmincon* optimization routine in Matlab.

### Code for fitting the pulse-based Cultivation

The mechanistic model of *E. coli* was solved in a pulsing manner to fit the data of the pulse-based scale-down cultivation. The pulsing scheme was determined by two time spans:  $t_{sp}$

and  $t_{swof}$ , which are respectively the times of glucose feed and glucose limitation. For each pulse cycle ( $t_{se} = t_{sp} + t_{swof}$ ), the exponential feed profile was integrated to find the volume of feed added within the time  $t_{sp}$ . The details of the calculations are given in the pseudocode in Algorithm A.1.

---

Algorithm A.1 Basic pseudocode of the pulsing scheme for exponential feeding phase

---

```

1   Define initial conditions :  $y_0 = [V_0 \ X_0 \ S_0 \ A_0 \ DOT_0]$  at the end of batch phase  $T_{start} = t_{batch}$ 
2   Set design variables:  $U = [\mu_{set} \ t_{se} \ t_{sp} \ S_i \ K_{La}]$ 
3   Specify parameter values for the mechanistic model:  $Par = [K_{ap} \ K_s \ qS_{max} \ pA_{max} \ Y_{px} \ \dots]$ 
4   Calculate initial feed rate:  $F_0 = \frac{\mu_{set}}{Y_x/S_i} V_0 X_0$ 
5   repeat {for  $k_1 = 1$ : number of pulse cycles}
6        $F_e = F_0 e^{\mu_{set} t_{se}}$  : Solve exponential feed for one pulse cycle:  $t_{se} = 0.167 \ h$ 
7       Calculate feed volume:  $V_F = \int_0^{t_{se}} F_e e^{\mu_{set} t_{se}} dt - \int_0^{t_{se}-1} F_0 e^{\mu_{set} t_{se}} dt$ 
8       Compute pulse flow rate:  $F_p = \frac{V_F}{t_{sp}}$ ,  $t_{sp}$  = pulse duration
9       Solve ODE system [Eqns A.1—A.15] for pulse duration with  $F_p$  as input,  $U(5) = K_{La\_low} \ rpm$ 
10       $[t_1 \ y_1] = ode15s (@fn\_Ecoli, t_{sp}, y_0, options, Par, F_p)$ 
11      if  $k_1 == 1$ 
12           $T = [T; t_1(1: end); Y = [Y; y_1(1: end).:]$ 
13      else
14           $T = [T; t_1(2: end); Y = [Y; y_1(2: end).:]$ 
15      end
16      Redefine initial conditions for glucose limitation phase:  $y_0 = Y(end, :)$ ,  $U(5) = K_{La\_high} \ rpm$ ,  $F_p = 0$ 
17       $t_{swof} = [T_{start} + t_{sp} \ T_{start} + t_{se}]$  = timespan of resting/glucose limitation phase
18       $[t_2 \ y_2] = ode15s (@fn\_Ecoli, t_{swof}, y_0, options, Par, F_p)$ 
19      if  $k_1 == 1$ 
20           $T = [T; t_2(1: end); Y = [Y; y_2(1: end).:]$ 
21      else
22           $T = [T; t_2(2: end); Y = [Y; y_2(2: end).:]$ 
23      end
24      Redefine initial conditions for next pulse:  $y_0 = Y(end, :)$ ,  $U(5) = K_{La\_low} \ rpm$ ,  $F_0 = F_e$ 
25  until {end} pulse cycles end

```

---

## REFERENCES

1. Neubauer P, Junne S. Scale up and scale down methodologies for bioreactors. In:

- Mandenius C-F, editor. *Bioreactors: Design, Operation and Novel Applications*. Wiley-VCH Verlag GmbH & Co. KGaA; 2016. p. 323–54.
2. Neubauer P, Cruz N, Glauche F, Junne S, Knepper A, Raven M. Consistent development of bioprocesses from microliter cultures to the industrial scale. *Eng Life Sci*. 2013;13(3):224–38.
  3. Neubauer P, Häggström L, Enfors S-O -O. Influence of substrate oscillations on acetate formation and growth yield in *Escherichia coli* glucose limited fed-batch cultivations. *Biotechnol Bioeng*. 1995 Jul 20;47(2):139–46.
  4. Bylund F, Castan A, Mikkola R, Veide A, Larsson G. Influence of scale-up on the quality of recombinant human growth hormone. *Biotechnol Bioeng*. 2000;69(2):119–28.
  5. Hewitt CJ, Nebe-von-Caron G, Axelsson B, McFarlane CM, Nienow AW. Studies related to the scale up of high cell density *E. coli* fed batch fermentations using multiparameter flow cytometry: Effect of a changing microenvironment with respect to glucose and dissolved oxygen concentration. *Biotechnol Bioeng*. 2000;70(4):381–90.
  6. Lara AR, Leal L, Flores N, Gosset G, Bolívar F, Ramírez OT. Transcriptional and metabolic response of recombinant *Escherichia coli* to spatial dissolved oxygen tension gradients simulated in a scale-down system. *Biotechnol Bioeng*. 2006;93(2):372–85.
  7. Neubauer P, Åhman M, Törnkvist M, Larsson G, Enfors SO. Response of guanosine tetraphosphate to glucose fluctuations in fed-batch cultivations of *Escherichia coli*. *J Biotechnol*. 1995;43(3):195–204.
  8. Lara AR, Taymaz-Nikerel H, Mashego MR, van Gulik WM, Heijnen JJ, Ramírez OT, et al. Fast dynamic response of the fermentative metabolism of *Escherichia coli* to aerobic and anaerobic glucose pulses. *Biotechnol Bioeng*. 2009;104(6):1153–61.
  9. Ying Lin H, Neubauer P. Influence of controlled glucose oscillations on a fed-batch process of recombinant *Escherichia coli*. *J Biotechnol*. 2000;79:27–37.
  10. Jaén KE, Sigala JC, Olivares-Hernández R, Niehaus K, Lara AR. Heterogeneous oxygen availability affects the titer and topology but not the fidelity of plasmid DNA produced by *Escherichia coli*. *BMC Biotechnol*. 2017;17(1):1–12.
  11. Limberg MH, Pooth V, Wiechert W, Oldiges M. Plug flow versus stirred tank reactor flow characteristics in two-compartment scale-down bioreactor: Setup-specific influence on the metabolic phenotype and bioprocess performance of *Corynebacterium glutamicum*. *Eng Life Sci*. 2016;16(7):610–9.

12. Li J, Jaitzig J, Lu P, Süßmuth RD, Neubauer P. Scale-up bioprocess development for production of the antibiotic valinomycin in *Escherichia coli* based on consistent fed-batch cultivations. *Microb Cell Fact.* 2015;14(1):1–13.
13. Lemoine A, Limberg MH, Kästner S, Oldiges M, Neubauer P, Junne S. Performance loss of *Corynebacterium glutamicum* cultivations under scale-down conditions using complex media. *Eng Life Sci.* 2016;1–13.
14. Sunya S, Bideaux C, Molina-Jouve C, Gorret N. Short-term dynamic behavior of *Escherichia coli* in response to successive glucose pulses on glucose-limited chemostat cultures. *J Biotechnol.* 2013;164(4):531–42.
15. Enfors SO, Jahic M, Rozkov A, Xu B, Hecker M, Jürgen B, et al. Physiological responses to mixing in large scale bioreactors. *J Biotechnol.* 2001 Feb 13;85(2):175–85.
16. Brand E, Junne S, Anane E, Cruz-Bournazou MN, Neubauer P. Importance of the cultivation history for the response of *Escherichia coli* to oscillations in scale-down experiments. *Bioprocess and Biosystems Engineering.* 2018 May 28;1–9.
17. Delvigne F, Takors R, Mudde R, van Gulik W, Noorman H. Bioprocess scale-up/down as integrative enabling technology: from fluid mechanics to systems biology and beyond. *Microb Biotechnol.* 2017 Sep;10(5):1267–74.
18. Haringa C, Tang W, Deshmukh AT, Xia J, Reuss M, Heijnen JJ, et al. Euler-Lagrange computational fluid dynamics for (bio)reactor scale down: An analysis of organism lifelines. *Eng Life Sci.* 2016;16(7):652–63.
19. Lapin A, Müller D, Reuss M. Dynamic Behavior of Microbial Populations in Stirred Bioreactors Simulated with Euler–Lagrange Methods: Traveling along the Lifelines of Single Cells. *Ind Eng Chem Res.* 2004;43(16):4647–56.
20. Wang G, Tang W, Xia J, Chu J, Noorman H, van Gulik WM. Integration of microbial kinetics and fluid dynamics toward model-driven scale-up of industrial bioprocesses. Vol. 15, *Engineering in Life Sciences.* 2015. p. 20–9.
21. Haringa C, Deshmukh AT, Mudde RF, Noorman HJ. Euler-Lagrange analysis towards representative down-scaling of a 22 m<sup>3</sup> aerobic *S. cerevisiae* fermentation. *Chem Eng Sci.* 2017;170:653–69.
22. Delvigne F, Lejeune A, Destain J, Thonart P. Modelling of the substrate heterogeneities experienced by a limited microbial population in scale-down and in large-scale bioreactors. *Chem Eng J.* 2006;120(3):157–67.
23. Baert J, Delepierre A, Telek S, Fickers P, Toye D, Delamotte A, et al. Microbial population heterogeneity versus bioreactor heterogeneity: Evaluation of Redox



- Sensor Green as an exogenous metabolic biosensor. *Eng Life Sci.* 2016;16(7):643–51.
24. Canelas AB, Ras C, ten Pierick A, van Gulik WM, Heijnen JJ. An in vivo data-driven framework for classification and quantification of enzyme kinetics and determination of apparent thermodynamic data. *Metab Eng.* 2011;13(3):294–306.
  25. Vanrolleghem PA, De Jong-Gubbels P, Van Gulik WM, Pronk JT, Van Dijken JP, Heijnen S. Validation of a metabolic network for *Saccharomyces cerevisiae* using mixed substrate studies. *Biotechnol Prog.* 1996;12(4):434–48.
  26. Cruz Bournazou MN, Barz T, Nickel DB, Lopez Cárdenas DC, Glauche F, Knepper A, et al. Online optimal experimental re-design in robotic parallel fed-batch cultivation facilities. *Biotechnol Bioeng.* 2017 Mar;114(3):610–9.
  27. Nickel DB, Cruz-Bournazou NM, Wilms T, Neubauer P, Knepper A. Online bioprocess data generation, analysis and optimization for parallel fed-batch fermentations at mL scale. *Eng Life Sci.* 2016;1–7.
  28. Hemmerich J, Noack S, Wiechert W, Oldiges M. Microbioreactor Systems for Accelerated Bioprocess Development. *Biotechnol J.* 2018;1700141:1–9.
  29. Barz T, Sommer A, Wilms T, Neubauer P, Cruz Bournazou MN. Adaptive optimal operation of a parallel robotic liquid handling station. *IFAC-PapersOnLine.* 2018;51(2):765–70.
  30. Junne S, Klingner A, Kabisch J, Schweder T, Neubauer P. A two-compartment bioreactor system made of commercial parts for bioprocess scale-down studies: Impact of oscillations on *Bacillus subtilis* fed-batch cultivations. *Biotechnol J.* 2011;6(8):1009–17.
  31. Anane E, López C DC, Neubauer P, Cruz Bournazou MN. Modelling overflow metabolism in *Escherichia coli* by acetate cycling. *Biochem Eng J.* 2017 Sep;125:23–30.
  32. Gao X, Kong B, Vigil RD. Characteristic time scales of mixing, mass transfer and biomass growth in a Taylor vortex algal photobioreactor. *Bioresour Technol.* 2015;198:283–91.
  33. Dörschug M, Habermann P, Seipke G, Uhlmann E. Mini-proinsulin , its production and use. Germany; EP0347781B1, 1988. p. 1–10.
  34. Jobé AM, Herwig C, Surzyn M, Walker B, Marison I, von Stockar U. Generally applicable fed-batch culture concept based on the detection of metabolic state by on-line balancing. *Biotechnol Bioeng.* 2003 Jun 20;82(6):627–39.
  35. Wong P, Gladney S, Keasling JD. Mathematical model of the lac operon: Inducer

- exclusion, catabolite repression, and diauxic growth on glucose and lactose. *Biotechnol Prog.* 1997;13(2):132–43.
36. Reitz C, Fan Q, Neubauer P. Synthesis of non-canonical branched-chain amino acids in *Escherichia coli* and approaches to avoid their incorporation into recombinant proteins. *Curr Opin Biotechnol.* 2018 Oct;53:248–53.
  37. Lin HY, Mathiszik B, Xu B, Enfors SO, Neubauer P. Determination of the maximum specific uptake capacities for glucose and oxygen in glucose-limited fed-batch cultivations of *Escherichia coli*. *Biotechnol Bioeng.* 2001;73(5):347–57.
  38. Xu B, Jahic M, Blomsten G, Enfors SO. Glucose overflow metabolism and mixed-acid fermentation in aerobic large-scale fed-batch processes with *Escherichia coli*. *Appl Microbiol Biotechnol.* 1999;51(5):564–71.
  39. Junker BH. Scale-up methodologies for *Escherichia coli* and yeast fermentation processes. *J Biosci Bioeng.* 2004 Jan;97(6):347–64.
  40. Bullwinkle T, Lazazzera B, Ibba M. Quality Control and Infiltration of Translation by Amino Acids Outside of the Genetic Code. *Annu Rev Genet.* 2014;48(1):149–66.
  41. Soini J, Falschlehner C, Liedert C, Bernhardt J, Vuoristo J, Neubauer P. Norvaline is accumulated after a down-shift of oxygen in *Escherichia coli* W3110. *Microb Cell Fact.* 2008;7(1):30.
  42. Morchain J, Gabelle J-C, Cockx A. A Coupled Population Balance Model and CFD Approach for the Simulation of Mixing Issues in Lab-Scale and Industrial Bioreactors. *AIChE J.* 2014;60:27–40.
  43. Larsson G, Törnkvist M, Ståhl Wernersson E, Trägårdh C, Noorman H, Enfors SO. Substrate gradients in bioreactors: Origin and consequences. *Bioprocess Eng.* 1996 May;14(6):281–9.
  44. Simen JD, Löffler M, Jäger G, Schäferhoff K, Freund A, Matthes J, et al. Transcriptional response of *Escherichia coli* to ammonia and glucose fluctuations. *Microb Biotechnol.* 2017;10(4):858–72.
  45. Marbà-Ardébol A-M, Emmerich J, Muthig M, Neubauer P, Junne S. Real-time monitoring of the budding index in *Saccharomyces cerevisiae* batch cultivations with in situ microscopy. *Microb Cell Fact.* 2018;17(1):73.

## Notation

$K_{ap}$  = Monod-type saturation constant, intracellular acetate prod. ( $\text{g g}^{-1} \text{h}^{-1}$ )

$K_{sa}$  = Affinity constant, acetate consumption ( $\text{g L}^{-1}$ )

$K_s$  = Affinity constant, glucose consumption ( $\text{g L}^{-1}$ )  
 $K_{ia}$  = Inhibition constant, inhibition of cellular growth by extracellular acetate ( $\text{g L}^{-1}$ )  
 $K_{is}$  = Inhibition constant, inhibition of acetate uptake by glucose ( $\text{g L}^{-1}$ )  
 $p_{Amax}$  = Maximum specific acetate production rate ( $\text{g g}^{-1} \text{h}^{-1}$ )  
 $q_{Amax}$  = Maximum specific acetate consumption rate ( $\text{g g}^{-1} \text{h}^{-1}$ )  
 $q_m$  = Specific maintenance coefficient ( $\text{g g}^{-1} \text{h}^{-1}$ )  
 $q_{Smax}$  = Maximum specific glucose uptake rate ( $\text{g g}^{-1} \text{h}^{-1}$ )  
 $Y_{as}$  = Yield of acetate on substrate ( $\text{g g}^{-1}$ )  
 $Y_{oa}$  = Specific oxygen used per gram of acetate metabolized ( $\text{g g}^{-1}$ )  
 $Y_{xa}$  = Yield of biomass on acetate ( $\text{g g}^{-1}$ )  
 $Y_{em}$  = Yield of biomass on glucose, excluding maintenance ( $\text{g g}^{-1}$ )  
 $Y_{os}$  = Oxygen used per gram of glucose metabolized per gram biomass ( $\text{g g}^{-1}$ )  
 $Y_{xsof}$  = Yield of biomass other products of overflow routes, excluding acetate ( $\text{g g}^{-1}$ )  
 $C$  = Carbon content of (s) substrate, (x) biomass  
 DOT = dissolved oxygen tension (%). DOT\* represents saturating value of DOT in the broth at the given operating conditions.  
 $F$  = Flow rate ( $\text{L h}^{-1}$ )  
 $\mu$  = specific growth rate ( $\text{h}^{-1}$ )